



# Chemical mutagenesis of a GPCR ligand: Detoxifying “inflammo-attraction” to direct therapeutic stem cell migration

Jean-Pyo Lee<sup>a,b,1,2</sup>, Runquan Zhang<sup>a,1</sup>, Maocai Yan<sup>a</sup>, Srinivas Duggineni<sup>a</sup>, Dustin R. Wakeman<sup>a</sup>, Walter L. Niles<sup>a</sup>, Yongmei Feng<sup>a</sup>, Justin Chen<sup>b</sup>, Milton H. Hamblin<sup>c</sup>, Edward B. Han<sup>d</sup>, Rodolfo Gonzalez<sup>a</sup>, Xiao Fang<sup>e</sup>, Yinsong Zhu<sup>e</sup>, Juan Wang<sup>e</sup>, Yan Xu<sup>e</sup>, David A. Wenger<sup>f</sup>, Thomas N. Seyfried<sup>g</sup>, Jing An<sup>h,2</sup>, Richard L. Sidman<sup>i,2</sup>, Ziwei Huang<sup>a,h,2,3</sup>, and Evan Y. Snyder<sup>a,j,2,3</sup>

<sup>a</sup>Center for Stem Cells and Regenerative Medicine, Sanford Burnham Prebys Medical Discovery Institute, La Jolla, CA 92037; <sup>b</sup>Department of Physiology, Tulane University School of Medicine, New Orleans, LA 70112; <sup>c</sup>Department of Pharmacology, Tulane University School of Medicine, New Orleans, LA 70112; <sup>d</sup>Department of Neuroscience, School of Medicine, Washington University in St. Louis, St. Louis, MO 63110; <sup>e</sup>School of Life Sciences, Tsinghua University, 100084 Beijing, China; <sup>f</sup>Department of Neurology, Jefferson Medical College, Philadelphia, PA 19107; <sup>g</sup>Biology Department, Boston College, Chestnut Hill, MA 02467; <sup>h</sup>Department of Medicine, University of California San Diego, La Jolla, CA 92037; <sup>i</sup>Department of Neurology, Harvard Medical School, Boston, MA 02115; and <sup>j</sup>Sanford Consortium for Regenerative Medicine, La Jolla, CA 92037

Contributed by Richard L. Sidman, April 5, 2020 (sent for review July 17, 2019; reviewed by Paul R. Sanberg, John R. Sladek Jr, and Young-sup Yoon)

**A transplanted stem cell's engagement with a pathologic niche is the first step in its restoring homeostasis to that site. Inflammatory chemokines are constitutively produced in such a niche; their binding to receptors on the stem cell helps direct that cell's "pathotropism." Neural stem cells (NSCs), which express CXCR4, migrate to sites of CNS injury or degeneration in part because astrocytes and vasculature produce the inflammatory chemokine CXCL12. Binding of CXCL12 to CXCR4 (a G protein-coupled receptor, GPCR) triggers repair processes within the NSC. Although a tool directing NSCs to where needed has been long-sought, one would not inject this chemokine in vivo because undesirable inflammation also follows CXCL12–CXCR4 coupling. Alternatively, we chemically "mutated" CXCL12, creating a CXCR4 agonist that contained a strong pure binding motif linked to a signaling motif devoid of sequences responsible for synthetic functions. This synthetic dual-moity CXCR4 agonist not only elicited more extensive and persistent human NSC migration and distribution than did native CXCL 12, but induced no host inflammation (or other adverse effects); rather, there was predominantly reparative gene expression. When co-administered with transplanted human induced pluripotent stem cell-derived hNSCs in a mouse model of a prototypical neurodegenerative disease, the agonist enhanced migration, dissemination, and integration of donor-derived cells into the diseased cerebral cortex (including as electrophysiologically-active cortical neurons) where their secreted cross-corrective enzyme mediated a therapeutic impact unachieved by cells alone. Such a "designer" cytokine receptor-agonist peptide illustrates that treatments can be controlled and optimized by exploiting fundamental stem cell properties (e.g., "inflammo-attraction").**

human induced pluripotent stem cells | neural stem cells | CXCR4 | neurodegeneration | homing

**A** transplanted stem cell's engagement with a pathologic niche is the first step in cell-mediated restoration of homeostasis to that region, whether by cell replacement, protection, gene delivery, milieu alteration, toxin neutralization, or remodeling (1–4). Not surprisingly, the more host terrain covered by the stem cells, the greater their impact. We and others found that a propensity for neural stem cells (NSCs) to home in vivo to acutely injured or actively degenerating central nervous system (CNS) regions—a property called “pathotropism” (1–12), now viewed as central to stem cell biology—is undergirded, at least in part, by the presence of chemokine receptors on the NSC surface, enabling them to follow concentration gradients of inflammatory cytokines constitutively elaborated by pathogenic processes and expressed by reactive astrocytes and injured vascular endothelium within the

pathologic niche (5–9). This engagement of NSC receptors was first described for the prototypical chemokine receptor CXCR4 (C-X-C chemokine receptor type 4; also known as fusin or cluster of differentiation-184 [CD184]) and its unique natural cognate agonist ligand, the inflammatory chemokine CXCL12 (C-X-C motif chemokine ligand-12; also known as stromal cell-derived factor 1α [SDF-1α]) (5), but has since been described for many chemokine receptor-agonist pairings (6–9). Chemokine receptors belong to a superfamily that is characterized by seven transmembrane GDP-binding protein-coupled receptors (GPCRs) (13–21). In addition to their role in mediating inflammatory reactions and immune responses (22, 23), these receptors and their

## Significance

**While inflammatory chemokines, constitutively produced by pathologic regions, are pivotal for attracting reparative stem cells, one would certainly not want to further “inflammo” a diseased brain by instilling such molecules. Exploiting the fact that receptors for such cytokines (G protein-coupled receptors [GPCR]) possess two “pockets”—one for binding, the other for signaling—we created a synthetic GPCR-agonist that maximizes interaction with the former and narrows that with the latter. Homing is robust with no inflammation. The peptide successfully directed the integration of human induced pluripotent stem cell derivatives (known to have muted migration) in a model of a prototypical neurodegenerative condition, ameliorating symptomatology.**

Author contributions: J.-P.L., R.Z., E.B.H., Y.X., J.A., R.L.S., Z.H., and E.Y.S. designed research; J.-P.L., R.Z., M.Y., S.D., D.R.W., W.L.N., Y.F., J.C., M.H.H., E.B.H., R.G., X.F., Y.Z., Y.X., D.A.W., and T.N.S. performed research; J.-P.L., R.Z., S.D., D.R.W., E.B.H., R.G., Y.X., D.A.W., T.N.S., R.L.S., Z.H., and E.Y.S. contributed new reagents/analytic tools; J.-P.L., R.Z., M.Y., W.L.N., Y.F., J.C., M.H.H., E.B.H., R.G., X.F., Y.Z., Y.X., D.A.W., T.N.S., J.A., R.L.S., Z.H., and E.Y.S. analyzed data; and J.-P.L., R.Z., J.A., R.L.S., Z.H., and E.Y.S. wrote the paper.

Reviewers: P.R.S., University of South Florida; J.R.S., University of Colorado School of Medicine; and Y-s.Y., Emory University.

Competing interest statement: J.R.S. was one of 17 coauthors with R.G. and E.Y.S. on a 2016 research article. He did not collaborate directly with them.

This open access article is distributed under [Creative Commons Attribution-NonCommercial-NoDerivatives License 4.0 \(CC BY-NC-ND\)](https://creativecommons.org/licenses/by-nc-nd/4.0/).

<sup>1</sup>J.-P.L. and R.Z. contributed equally to this work.

<sup>2</sup>To whom correspondence may be addressed. Email: esnyder@sbc.edu, zhuang@health.ucsd.edu, jeanpyol@tulane.edu, jan@health.ucsd.edu, or richard\_sidman@hms.harvard.edu.

<sup>3</sup>Z.H. and E.Y.S. contributed equally to this work.

This article contains supporting information online at <https://www.pnas.org/lookup/suppl/doi:10.1073/pnas.1911444117/-DCSupplemental>.

First published November 20, 2020.

CELL BIOLOGY

agonists are components of the regulatory axes for hematopoiesis and organogenesis in other systems (21, 24). Therefore, it is not surprising that binding of CXCL12 to CXCR4 mediates not only an inflammatory response, but also triggers within the NSC a series of intracellular processes associated with migration (as well as proliferation, differentiation, survival, and, during early brain development, proper neuronal lamination) (10).

A tool directing therapeutic NSCs to where they are needed has long been sought in regenerative medicine (11, 12). While it was appealing to contemplate electively directing reparative NSCs to any desired area by emulating this chemoattractive property through the targeted injection of exogenous recombinant inflammatory cytokines, it ultimately seemed inadvisable to risk increasing toxicity in brains already characterized by excessive and usually inimical inflammation from neurotraumatic or neurodegenerative processes. However, the notion of engaging the homing function of these NSC-borne receptors without triggering that receptor's undesirable downstream inflammatory signaling [particularly given that the NSCs themselves can exert a therapeutic antiinflammatory action in the diseased region (1, 2)] seemed a promising heretofore unexplored "workaround."

There had already been an impetus to examine the structure–function relationships of CXCR4, known to be the entry route into cells for HIV-1, in order to create CXCR4 antagonists that block viral infection (25–30). Antagonists of CXCR4 were also devised to forestall hematopoietic stem cells from homing to the bone marrow, hence prolonging their presence in the peripheral blood (31) to treat blood dyscrasias. An agonist, however, particularly one with discrete and selective actions, had not been contemplated. In other words, if CXCL12 could be stripped of its undesirable actions while preserving its tropic activity, an ideal chemoattractant would be derived.

Based on the concept that CXCR4's functions are conveyed by two distinct molecular "pockets"—one mediating binding (i.e., allowing a ligand to engage CXCR4) and the other mediating signaling (i.e., enabling a ligand, after binding, to trigger CXCR4-mediated intracellular cascades that promote not only inflammation but also migration) (13–18)—we performed chemical mutagenesis that should optimize binding while narrowing the spectrum of signaling. We created a simplified de novo peptide agonist of CXCR4 that contained a strong pure binding motif derived from CXCR4's strongest ligand, viral macrophage inflammatory protein-II (vMIP-II) and linked it to a truncated signaling motif (only 8 amino acid residues) derived from the N terminus of native CXCL12 (19, 20). This synthetic dual-moiety CXCR4 agonist, which is devoid of a large portion of CXCL12's native sequence (presumably responsible for undesired functions such as inflammation) not only elicited (with great specificity) more extensive and long-lasting human NSC (hNSC) migration and distribution than native CXCL12 (overcoming migratory barriers), but induced no host inflammation (or other adverse effects). Furthermore, because all of the amino acids in the binding motif were in a D-chirality, rendering the peptide resistant to enzymatic degradation, persistence of this benign synthetic agonist *in vivo* was prolonged. The hNSC's gene ontology expression profile was predominantly reparative in contrast to inflammatory as promoted by native CXCL12. When coadministered with transplanted human induced pluripotent stem cell (hiPSC)-derived hNSCs (hiPSC derivatives are now known to have muted migration) in a mouse model of a prototypical neurodegenerative disease [the lethal neuropathic lysosomal storage disorder (LSD) Sandhoff disease (29), where hiPSC-hNSC migration is particularly limited], the synthetic agonist enhanced migration, dissemination, and integration of donor-derived cells into the diseased cortex (including as electrophysiologically active cortical neurons), where their secreted cross-corrective enzyme could mediate a histological and functional

therapeutic impact in a manner unachieved by transplanting hiPSC-derived cells alone.

In introducing such a "designer" cytokine receptor agonist, we hope to offer proof-of-concept that stem cell-mediated treatments can be controlled and optimized by exploiting fundamental stem cell properties (e.g., "inflammo-attraction") to alter a niche and augment specific actions. Additionally, when agonists are strategically designed, the various functions of chemokine receptors (and likely other GCPRs) may be divorced. We demonstrate that such a strategy might be used safely and effectively to direct cells to needed regions and broaden their chimerism. We discuss the future implications and uses within the life sciences of such a chemical engineering approach.

## Results

### Designing a Synthetic "Purely" Chemoattractant CXCR4 Agonist.

CXCL12 is comprised of an N-loop, a 30's loop, and an anti-parallel  $\beta$ -sheet with three  $\beta$ -strands adjacent to a C-terminal  $\alpha$ -helix. It is thought that the N terminus of CXCL12's globular core structure engages CXCR4 and is mainly responsible for both binding to CXCR4 and triggering its signaling (13–16) (Fig. 1). Studies by many groups, including our own, have suggested that CXCR4 possesses two different "pockets" within its seven-transmembrane helices with which CXCL12 interacts: One mediating binding, the other signaling (13–19, 25–27). In a complimentary manner, two different regions of CXCL12's N terminus, respectively, engage each CXCR4 pocket independently, first binding and then signaling (19–21, 24–27). Based on this model, we designed (as detailed below and schematized in Fig. 1B) CXCL12 "mimics" that might be solely "promigratory" by inserting CXCR4's strongest binding motifs but retaining only the most minimal and selective of signaling sequences (Figs. 1B and 2 A and B).

We began by choosing a high-affinity binding motif. Recognizing that the strongest "binder" to CXCR4 is actually its antagonist, the viral chemokine vMIP-II that stimulates no signaling activity (28) (Fig. 2B), we substituted vMIP-II's receptor binding sequence (located at its N terminus) for CXCL12's corresponding natural binding motif (Fig. 1B). To determine the proper vMIP-II residues, we performed a series of CXCR4 *in silico* molecular docking studies analyzing the interaction between CXCR4 and different small 21-mer all-D-chirality amino acid peptide derivatives of the N-terminal residue of vMIP-II, creating a family of synthetic ligands (collectively called "DV"), each with a different D-(1~21)-vMIP-II binding moiety (Fig. 24). The various peptides were modeled making contact with the binding and signaling pockets of CXCR4 using computational methods (32–35) to determine which made maximal contact with the former without binding the latter. One DV family member was selected, DV1, based on its energy-favorable initial-stage docking profile. Over a 5-ns molecular dynamics (MD) simulation, backbone atoms of both the ligand and the receptor showed consistently lower RMSD (i.e., small RMS fluctuations) (Fig. 2 A, a), denser hydrogen bond formation (Fig. 2 A, b and d), and stronger electrostatic and van der Waals interactions at the binding pocket compared to the signaling pocket (Fig. 2 A, c). Specifically, at the binding pocket, Leu1 of DV1 formed hydrogen bonds with Tyr256 and Glu288 of CXCR4; Gly2, Ala3, and Ser4 of DV1 formed many hydrogen bonds with Glu288 of CXCR4; Ala3 also formed a hydrogen bond with Gln272. Arg7 of DV1 formed three hydrogen bonds with Ala98 and Trp102 of CXCR4 (Fig. 2 A, d, Left). There were also many hydrophobic interactions between DV1 and CXCR4; for example, Leu1 of DV1 with Tyr116 and Tyr256 of CXCR4, Ala3 of DV1 with Ser285 of CXCR4, and Trp5 of DV1 with Tyr103, Phe104, Tyr184, Phe189 of CXCR4; Pro8 of DV1 with Cys28 of CXCR4 (Fig. 2 A, d, Left). These findings indicated a more favorable and selective interaction between DV1 and CXCR4's binding pocket

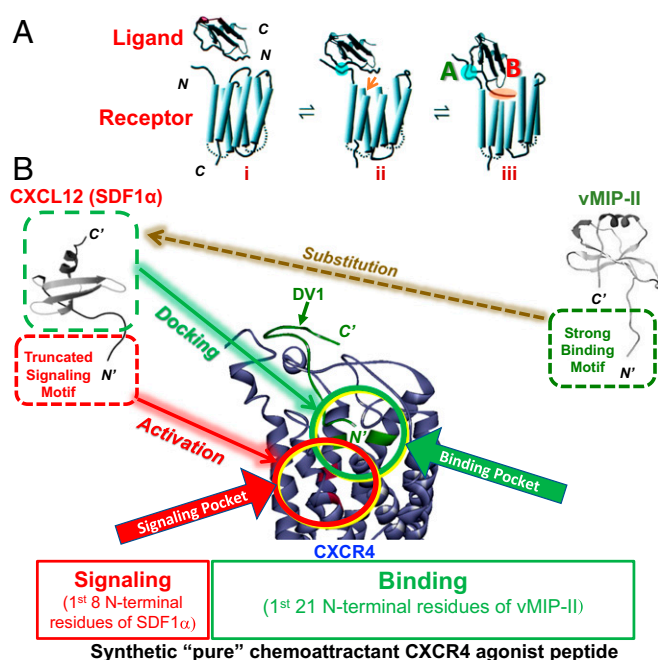


**Fig. 1.** Design of a synthetic purely chemoattractant CXCR4 agonist. (A) Normally, the intact chemokine agonist CXCL12 (also known as SDF1 $\alpha$ ) binds to its receptor, CXCR4, in two steps to two different pockets, respectively. After initial binding of the proximal N terminus of CXCL12's globular core structure to the binding pocket in CXCR4's extracellular transmembrane regions, CXCL12's distal N terminus reaches CXCR4's transmembrane signaling pocket and leads to allosteric modulation of CXCR4's conformation which, in turn, enables canonical receptor functions, including activating multiple downstream G protein-mediated signaling pathways (adapted with permission from ref. 13). (B) Strategy for synthesizing SDV1a, a dual-moiety bifunctional hNSC chemoattractant with maximal binding and negligible inflammatory, yet preserved reparative stem cell-related signaling. The first 21 amino acids (all in a D-chirality) from the N terminal of the CXCR4 antagonist vMIP-II, were inserted in place of CXCL12's proximal N terminus in order to provide a ligand with the highest possible affinity for the binding pocket (green circle); it promotes no signaling (Fig. 2D). It was called DV1. The distal N-terminal signaling motif of CXCL12, which engages the signaling pocket (red circle), was truncated to the first 8 amino acids (including the first 2 amino acids required for signaling) in order to narrow the spectrum of G protein-mediated pathways activated to those supportive of cell proliferation, migration, and survival (e.g., MAPK) while excluding (or minimizing) those involved in inflammatory cascades (SI Appendix, Figs. S4, S6, and S7). This truncated signaling motif was called S1. Therefore, the designer peptide was designated L-(1~8)-SDF1 $\alpha$ -GG-D-(1~21)-vMIP-II, or SDV1a for short.

than with its signaling pocket, an encouraging basis for the dual-moiety agonist we were attempting to design.

Because the N terminus of DV1 would now form fewer polar interactions with CXCR4's signaling pocket than does native CXCL12 (Fig. 2 A, d, Right), that pocket could now become available, after DV1 binding, for interactions with a separate signaling motif from the environment, and hence potentially activate unintended and undesirable full signaling. Accordingly, the next step in our design was to occupy that signaling pocket but do so by using the signaling portion of the N terminus of native CXCL12 truncated from a 68-mer to merely an 8-mer peptide [that nevertheless retained the first 2 amino acid residues, which are essential for signaling (13, 14)]. Therefore, this shortened peptide, which we called S1, could occupy CXCR4's signaling pocket but narrow the spectrum of CXCR4 signaling. Because DV1 was positioned and synthetically coupled to the C-terminal end of S1, this new hybrid peptide was called SDV1.

To ensure an appropriate spatial arrangement of the two linked peptide moieties for optimally performing their respective binding and signaling functions, different spacer sequences were inserted between them, yielding three candidates—designated SDV1a, SDV1b, and SDV1c—which might serve as our new bifunctional agonist (see SI Appendix, Table S1 for sequences). These candidates were synthesized, their purity confirmed with high-performance liquid chromatography, and their molecular weights validated by matrix-assisted laser desorption/ionization-time of flight mass spectrometry (SI Appendix, Fig. S1).

**Chemical and Molecular Characterization of the Synthetic CXCR4 Agonists.** We next determined the CXCR4-selective binding efficiency of these candidates by comparing their ability to outcompete the binding of a fluorophore-conjugated anti-CXCR4-specific monoclonal antibody (Clone 12G5) to cells that highly express CXCR4 and are the literature's standard for CXCR4-expressing cells (the Sup-T1 human lymphoma T-cell line) (28). All three peptides exhibited high CXCR4-binding potency in this 12G5-based competitive receptor binding assay (SI Appendix, Fig. S2A) with an IC<sub>50</sub> ranging from lower micromolar to submicromolar concentrations (SI Appendix, Fig. S2B), a bit less than the antagonist DV1 alone but greater than the S1 truncated signaling portion alone.

Next, we evaluated the candidates' relative signaling capacities. As with other GPCRs, binding of an agonist to CXCR4 causes a catalytic exchange of GDP for GTP by dissociation of the G protein's linked trisubunits; the G  $\alpha$ -subunit regulates cell surface receptor dynamics, while the G  $\beta$ - and  $\gamma$ -subunits regulate MAPK signaling via the gating of intracellular calcium (Ca<sup>2+</sup><sub>i</sub>) (7) [which, in turn, controls other intracellular second messengers, e.g., IP<sub>3</sub> and cAMP (21)]. We, therefore, measured the dose-dependent Ca<sup>2+</sup> efflux kinetics of Sup-T1 cells treated with these synthetic "dual-moiety" CXCR4-binding peptides. Signaling amplitude was probed with a dual-wavelength Ca<sup>2+</sup> indicator Fura-2/AM using ratiometric conversions of Ca<sup>2+</sup> concentrations inside the cytosolic environment (Fig. 2B and SI Appendix, Fig. S2C). Measurements were made using a fluorescence plate-reader facilitated by an automated liquid handling system. Both SDV1a and SDV1c (but not SDV1b) elevated Ca<sup>2+</sup> efflux with increasing concentrations (SI Appendix, Fig. S2 C, ii), implying activation of MAPK signaling, which leads to a cascade of multiple downstream intracellular events, including but not limited to cell motility (36, 37). The amount of Ca<sup>2+</sup> efflux (i.e., signaling), however, was dramatically less than the signaling induced by natural CXCL12, one of our goals (SI Appendix, Fig. S2 C, i). In contrast, SDV1a's truncated "signaling moiety" (S1) alone required a 100-fold greater concentration than natural CXCL12 and a 10-fold greater concentration than SDV1a to elicit comparable Ca<sup>2+</sup> release (SI Appendix, Fig. S2 C, iii). The "binding moiety" alone from antagonist vMIP-II (DV1), as expected, evoked no signaling, even at concentrations as high as 40  $\mu$ M (SI Appendix, Fig. S2 C, iii).

**Impact on Cells of Candidate Synthetic CXCR4 Agonists.** Finally, we assessed the candidates' relative capacities to promote cellular migration using a Boyden chamber chemotaxis assay. With a porous (8  $\mu$ m) membrane separating the upper from the lower chamber, Sup-T1 cells were placed in the former and the candidate peptides (at titrated concentrations) placed in the latter (SI Appendix, Fig. S2D, schematic). (Note: hNSCs replaced Sup-T1 cells in subsequent experiments once a candidate was selected). Dose-dependent cell migration from the upper to the lower chamber was elicited by all three bifunctional peptide candidates (SI Appendix, Fig. S2D) (S1 and DV1, as expected, elicited no chemotaxis). Preincubation of the cells with the CXCR4-specific blocking antibody 12G5 suppressed migration, suggesting that CXCR4 was mediating this response. As an additional control, in

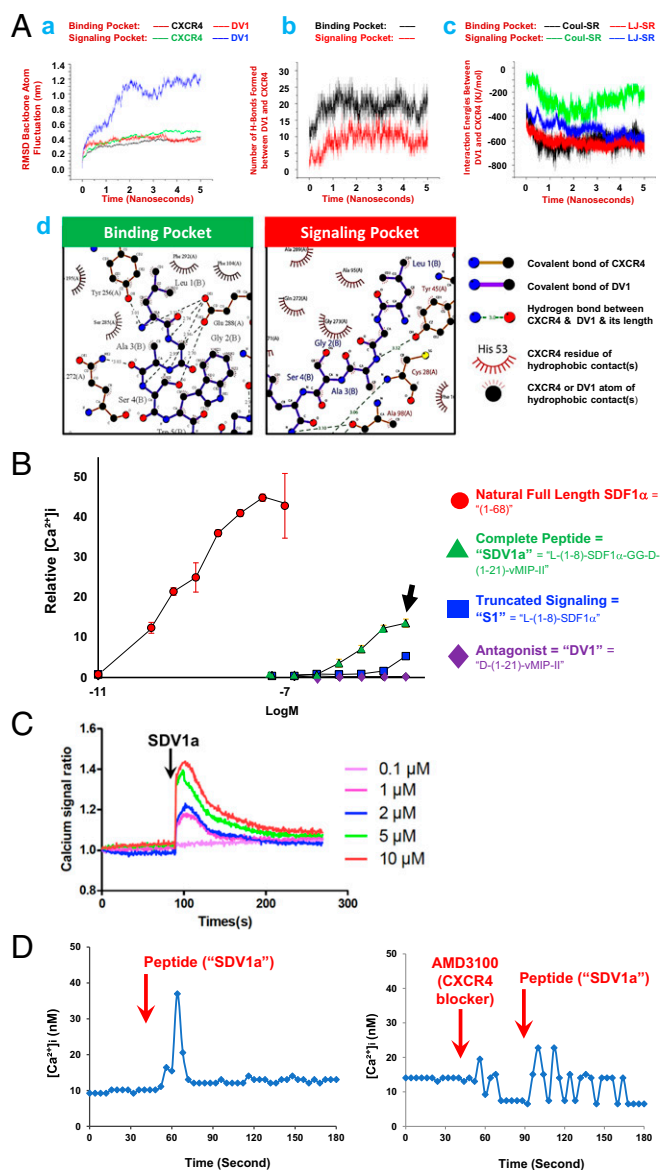


**Fig. 2.** Chemical and molecular characteristics of the synthetic CXCR4 agonist peptide SDV1a. (A) MD simulation in silico of interactions between the synthetic binding peptide DV1 and CXCR4. Briefly, a CXCR4 homology model was constructed and docking simulations were performed among 60 potential peptides derived from vMIP-II. The most energy-favorable candidates were chosen, as illustrated here for DV1 (the one ultimately selected). MD simulations (5 ns) of this complex with CXCR4 were then performed. (a) RMSD analysis of backbone atoms of CXCR4 and DV1 showing their fluctuations over time. It is greater at the binding site. (b) Number of hydrogen (H-) bonds formed between DV1 and CXCR4 over time. More are formed at the binding site. (c) Electrostatic (Coul-SR) and van der Waals (LJ-SR) interaction energies between DV1 and CXCR4. These are stronger at the binding site. (d) Two-dimensional Ligplot results showing that the N-terminal residues of DV1 form more polar interactions with CXCR4 at the binding pocket (Left) than at the signaling pocket (Right) by the end of the simulation. (B) SDV1a induces modulated signaling. Because activation of  $Ca^{2+}$  efflux is downstream of GPCR activation of  $Ca^{2+}$  channels,  $Ca^{2+}$  mobilization assays can serve as surrogates for signaling. Shown is ratiometric  $[Ca^{2+}]_i$  release from the literature's standard CXCR4-expressing cell line, Sup-T1, as measured by Fura-2/AM fluorescence intensity following treatment with: 1) Full-length CXCL12/SDF1 $\alpha$  (red circle), 2) SDV1a (green triangle), or 3) the components of SDV1a in isolation, its binding motif (derived from the antagonist vMIP-II [DV1]) (purple square) and its truncated signaling motif (S1) (blue triangle). As expected, the natural agonist CXCL12/SDF1 $\alpha$  produced the most intense signaling, while the antagonist produced none. When S1 was combined with DV1, however, to create SDV1a,

some conditions a test candidate was added to the upper chamber or to both chambers; the greatest migration was observed when the peptide was present only in the lower chamber, suggesting chemotaxis (rather than spontaneous random cell motility) as the predominant mechanism for transmigration of the cells (*SI Appendix, Fig. S2 D, Right Inset*). Based on efficiency of binding, potency in eliciting cell migration yet modulated degree of MAPK signaling, we chose SDV1a as the bifunctional dual moiety synthetic peptide agonist for use in all subsequent in vitro and in vivo experiments involving hNSCs with an eye toward translational applications.

**Impact on hNSCs of the Synthetic CXCR4 Agonist Peptide SDV1a.** Although previously documented (8), we reconfirmed abundant expression of CXCR4 on primary fetal brain-derived hNSCs (1–3, 5, 38, 39) (*SI Appendix, Fig. S3*). We next determined whether SDV1a's actions on hNSCs were comparable to those of CXCL12 (5). First, we investigated whether SDV1a triggered the same intracellular CXCR4-mediated downstream signaling cascades as CXCL12 (5). Western blot analysis was performed on lysates from hNSCs prestimulated with either SDV1a or CXCL12 to assess changes in the phospho-kinetics of several cardinal proteins downstream of CXCR4 (*SI Appendix, Fig. S4*). As with CXCL12, we observed rapid (within 2 to 5 min) phosphorylation (at Tyr202 and Tyr204) of the extracellular signal-regulated kinases 1/2 (ERK1/2) by SDV1a, suggesting that, in subsequent experiments, we should expect to see—as we did with CXCL12 (5)—induction of such relevant ERK1/2-downstream activities as cell motility (5, 36, 40) (*SI Appendix, Fig. S4 A and B*). Also phosphorylated were p38-MAPK (at Thr180/Tyr182) and I $\kappa$ B $\alpha$  (inhibitor of NF- $\kappa$ B  $\alpha$ ) (at Ser-32/36) (*SI Appendix, Fig. S4C*), as we previously reported for CXCL12's action on the very same hNSC clones (5). It is telling that these “reparative” cascades within hNSCs could be triggered despite the fact that signaling following SDV1a exposure, as assayed by  $Ca^{2+}$  efflux, was an order-of-magnitude less than following recombinant CXCL12 exposure (Fig. 2B and *SI Appendix, Fig. S5*). SDV1a's action (which is dose-dependent) (Fig. 2C) was blocked by pretreatment of the hNSCs with AMD3100, a small-molecule CXCR4-specific inhibitor (which desensitizes CXCR4 to agonist activation) (31), confirming a CXCR4-specific mechanism of action (Fig. 2D and *SI Appendix, Fig. S5*).

ideally modulated signaling was obtained (an order-of-magnitude less than CXCL12/SDF1 $\alpha$ ), yielding an optimal signaling profile. (See *SI Appendix, Fig. S2C* for an expanded presentation of these data, and *SI Appendix, Figs. S4 and S6* for the molecular consequences of this signaling.) These findings, taken together with SDV1a's also having the strongest affinity for CXCR4 among the candidates (*SI Appendix, Fig. S2B*), led to SDV1a's use in all subsequent experiments, particularly those performed in vivo. Shown are the mean values of three technical replicates from one of at least three independent biological replicates. Error bars represent  $\pm$  SEM. (C) Effect of different SDV1a doses on CXCR4-mediated  $Ca^{2+}$  mobilization (efflux). SDV1a triggered a typical  $Ca^{2+}$  spike in CXCR4-expressing cells in a dose-dependent manner. The EC<sub>50</sub> of calcium efflux was between 2 and 5  $\mu$ M, consistent with its binding IC<sub>50</sub> (as per *SI Appendix, Fig. S2B*). (D) Blocking CXCR4 inhibits activation of  $Ca^{2+}$  signaling by SDV1a. See *SI Appendix, Fig. S5* for experimental details and an expanded presentation of these data, including from other control conditions. Briefly, single hNSCs, loaded with Fura-2/AM, were measured for a 340/380 ratio of free  $[Ca^{2+}]_i$ . Calculated changes in  $[Ca^{2+}]_i$  were expressed in arbitrary units. A peak was defined as a fluorescence ratio increase at least three times greater than the noise level for the same cell. SDV1a (10  $\mu$ M) increased  $[Ca^{2+}]_i$  (Left), whereas AMD3100 (100  $\mu$ M), a CXCR4-specific blocker, reduced the  $[Ca^{2+}]_i$ , if added just prior to SDV1a exposure (Right), even at SDV1a's highest dose (as determined in C). Each panel shows the result of a single cell's transient  $[Ca^{2+}]_i$  release but represents the results of at least 11 cells per condition.

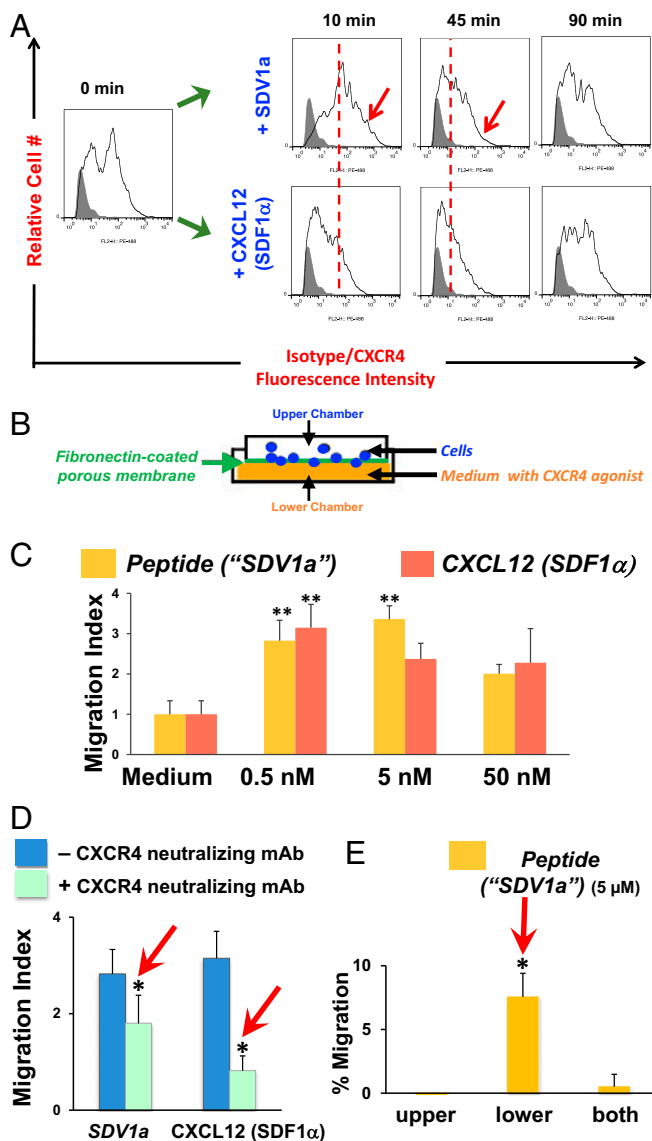


**Fig. 3.** Impact on hNSCs of the synthetic CXCR4 agonist peptide SDV1a. (A) Flow cytometric analysis of CXCR4 surface expression, endocytosis, and recycling in hNSCs activated by SDV1a vs. CXCL12/SDF1 $\alpha$  over time. As shown in this receptor endocytosis analysis, when bound by either ligand (4  $\mu$ g/mL), there was a dynamic recycling of cell surface CXCR4. However, the kinetics of endocytosis of CXCR4 was slower in response to SDV1a, taking 90 min to down-regulate (Upper). In contrast, CXCL12 binding induced down-regulation of CXCR4 expression on the hNSC surface rapidly, within the first 10 min; cell surface CXCR4 did not start to rebound until after 45 min (Lower). This difference meant that the surface expression of CXCR4 on hNSCs was more prolonged following binding by SDV1a than by natural CXCL12 (red arrows, Upper), suggesting that hNSCs may be poised to experience a more protracted chemoattractive pull from the synthetic agonist. Furthermore, as endocytosis of GPCRs is required for canonical G protein- and  $\beta$ -arrestin-mediated CXCR4 signaling, this finding of longer cell surface expression of CXCR4 and quicker surface reexpression (i.e., a shorter time spent intracellularly) may also contribute to muting certain undesirable downstream actions of CXCR4 within these hNSCs (e.g., minimizing GPCR-mediated inflammatory cascades). (B–E) In assays comparing their chemoattractive actions upon hNSCs, SDV1a matched the efficacy of native CXCL12 (SDF1 $\alpha$ ). (B) A Boyden chamber transmigration assay was used in which hNSCs ( $1 \times 10^5$  in 100  $\mu$ L medium) were placed in the upper chamber and the agent to be tested (in 600  $\mu$ L medium) was placed in the bottom chamber. The chambers were separated by a 6.5-mm-diameter 8- $\mu$ m pore-size transwell insert coated with fibronectin (1  $\mu$ g/cm $^2$ ). After 5 h of incubation, hNSCs that had migrated from the upper to the lower chamber and attached to the bottom of the transwell insert were fixed, stained with Crystal violet, and

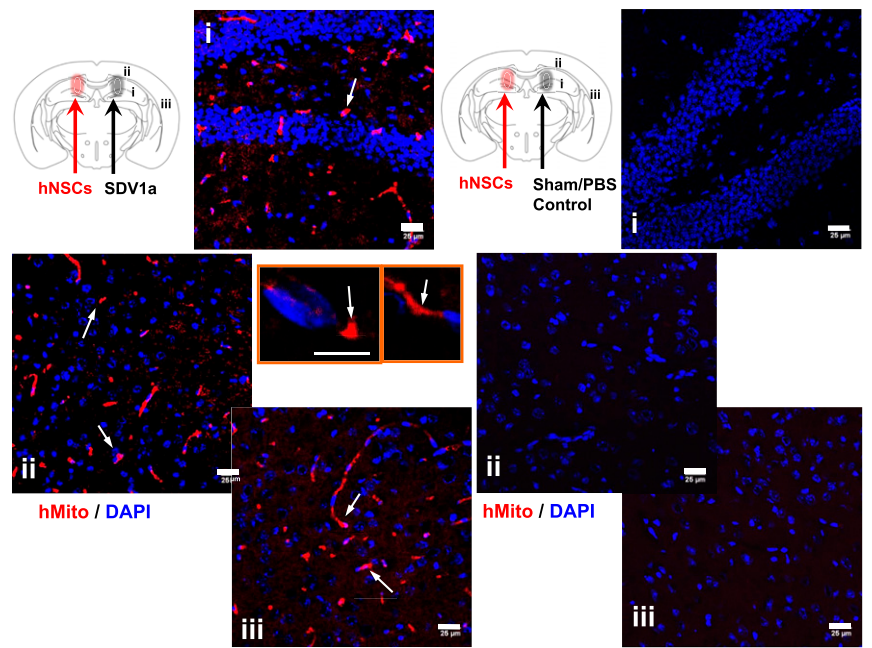
We next used flow cytometry (FACS) of live hNSCs to monitor the dynamics of CXCR4 cell surface expression (i.e., the kinetics of receptor endocytosis and reappearance) following ligand binding (41), comparing SDV1a with CXCL12. Under both conditions, there was a transient elevation followed by a down-regulation of CXCR4 surface expression; however, the kinetics of this endocytosis/reexpression cycle differed for the two ligands. CXCR4 recycling was slower and surface expression more persistent following SDV1a stimulation (Fig. 3 A, Upper) than following CXCL12 induction (Fig. 3 A, Lower), suggesting that hNSCs may be poised to experience a more protracted chemoattractive “pull” from the synthetic agonist. Furthermore, as endocytosis of GPCRs is required for canonical G protein and  $\beta$ -arrestin-mediated CXCR4 signaling, this finding of longer cell surface expression of CXCR4 and quicker surface reexpression may also contribute to our goal of muting certain undesirable downstream actions of CXCR4 that occur intracellularly (e.g., minimizing GPCR-mediated inflammatory cascades) in favor of reparative ones.

To explore this possibility further, differential gene-expression analysis using gene ontology terms was performed on hNSCs exposed to SDV1a compared to those exposed to CXCL12. As expected, there was some overlap in regulated genes (SI Appendix, Fig. S6 A and B). Under both conditions, the most highly ranked genes were those involved in cytoskeleton reorganization, (e.g., regulation of cell cycle, adhesion and proliferation, keratin filament formation, and epithelial-to-mesenchymal transition). But, also telling were differences in the hierarchy of cellular events promoted: Prominent in hNSCs treated with CXCL12 was up-regulation of inflammatory and immune-related processes, such as IFN- $\alpha/\beta$  signaling, stimulation of arachidonic acid production, and hypoxia-related functions, which were not prominent following treatment with SDV1a (SI Appendix, Fig. S6C). Rather, SDV1a primarily induced genes associated with developmental, homeostatic, and stem cell-related functions (SI Appendix, Fig. S7). (A detailed study of the molecular regulation of the multiple GPCR-mediated downstream pathways implicated is beyond the scope of the present paper.)

We next determined SDV1a’s action on actual hNSC behavior. We had previously reported (8) that exposure of hNSCs to CXCL12 and the consequent induction of CXCR4-mediated signaling triggers a series of intracellular processes associated

counted. A migration index was calculated by comparing the number of cells that migrated in response to a test chemoattractant peptide vs. to medium alone. (C) The migratory index of hNSCs confronted with SDV1a was similar to that for CXCL12/SDF1 $\alpha$  in a Boyden chamber. Both agonists produced a typical bell-shaped dose-response, with chemotaxis peaking at 5 nM for SDV1a and at 0.5 nM for CXCL12, consistent with their 10-fold differences in signaling intensity. Results shown represent the mean values at least two independent biological replicates, each with three technical replicates per experiment (\*\* $P < 0.05$ , one-tailed Student’s  $t$  test,  $\pm$  SEM). (See SI Appendix, Fig. S2D for an expanded presentation of these data with additional experimental conditions.) (D) Preincubation of the hNSCs with the CXCR4-specific blocking antibody 12G5 suppressed the promigratory actions of both CXCL12 and SDV1a, suggesting that CXCR4 binding and activation were mediating the chemoattractive actions for both agents. Results shown represent the mean values at least two independent biological replicates, each with three technical replicates per experiment (\* $P < 0.05$ , one-tailed Student’s  $t$  test,  $\pm$  SEM). (E) hNSCs migrated in response to a SDV1a concentration gradient based on chemoattraction and not spontaneous random cell motility. hNSCs seeded into the top chamber of the Boyden chamber (B) preferentially migrate toward SDV1a added into the lower chamber (creating a concentration gradient) as opposed to its being added into the upper chamber or into both chambers (abrogating an SDV1a concentration gradient). Results represent at least two independent biological replicates, each with three technical replicates per experiment ( $\pm$ SD) (\* $P < 0.05$ ). See SI Appendix, Fig. S2D for additional experimental conditions.

**Fig. 4.** Transplanted hNSCs are drawn to SDV1a across large distances in the adult mammalian brain. WT intact adult (6- to 8-wk old) C57BL/6J mice were implanted (by stereotaxic guidance to the location indicated in the schematics) with hNSCs (2  $\mu$ L from a  $1 \times 10^5$  cells/ $\mu$ L dissociated cell suspension) contemporaneously with injections (into the three contralateral regions indicated in the schematics) of either SDV1a (*Left*) or PBS (sham control) (*Right*). (*i* = hippocampus; *ii* and *iii* = two different regions of cortex). Coronal sections (20  $\mu$ m) were analyzed immunohistochemically from each region to detect hNSCs that had migrated from the opposite hemisphere, using the well-established hMito (red) (1) at various time intervals posttransplant, ranging from 2 wk (shown here) to 4 mo. See *Insets* for magnified images hNSC-derived hMito-immunopositive cells (red), demonstrating their unambiguous cytoplasmic appearance in relation to DAPI<sup>+</sup> nuclei (blue). With the exception of the rostral migratory stream, the intact adult rodent brain does not usually support long-distance migration of NSCs in the cerebrum. However, as shown, *Left*, transplanted hNSCs migrated to the multiple contralateral regions injected with SDV1a. No such migration occurred when PBS was injected into regions *i* to *iii*; no hNSCs were evident there (*Right*), an appearance identical, as well, to that following injection of recombinant CXCL12 into those regions (see section of text entitled *Transplanted hNSCs Are Drawn to SDV1a across Large Distances in the Adult Brain* for explanation). (Scale bars, 25  $\mu$ m.) (Data from mice who received injections of SDV1a without hNSCs are shown in *SI Appendix, Fig. S8.*)



with fundamental aspects of stem cell proliferation and migration. Would SDV1a do the same?

With regard to proliferation, SDV1a (10 nM), when added for 72 h to hNSCs in a CyQuant proliferation assay, increased total DNA content by 10% compared to untreated controls, similar to the effect of recombinant human CXCL12 protein. In the above-described Boyden chamber assay of chemotaxis (Fig. 3*B*), the promigratory actions of SDV1a were indistinguishable from those of CXCL12, both evincing a typical bell-shaped dose-dependence, with chemotaxis peaking at 5 nM for SDV1a and at 0.5 nM for CXCL12 (Fig. 3*C*). Preincubation of the hNSCs with the above-mentioned CXCR4-specific blocking antibody 12G5 abrogated the promigratory actions of both ligands (Fig. 3*D*), suggesting that CXCR4 binding and activation were mediating the chemoattraction for both agents. Again, as an additional control, SDV1a was added to the upper chamber (where the hNSCs were seeded) or to both chambers (abrogating a concentration gradient); hNSC migration (upper to lower chamber) was observed only when SDV1a was present in the lower chamber, implicating chemotaxis (rather than solely spontaneous random cell motility) as the likely mechanism for hNSC transmigration in response to SDV1a (Fig. 3*E*).

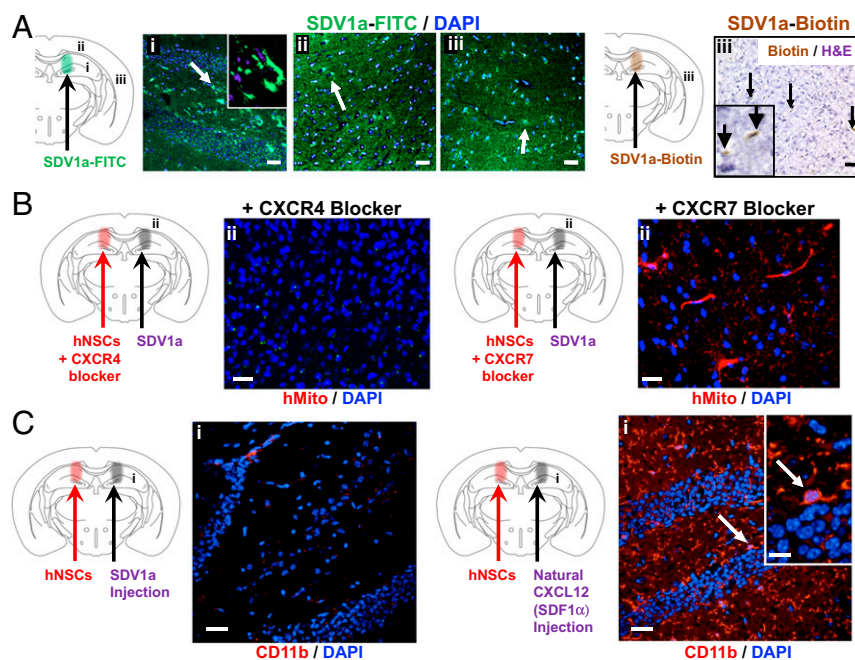
**Transplanted hNSCs Are Drawn to SDV1a across Large Distances in the Adult Brain.** Based on SDV1a's actions on hNSCs in vitro (compared to those of CXCL12), we expected that, if administered in vivo, SDV1a would attract transplanted hNSCs as efficiently as we reported for naturally expressed CXCL12 (5) but without provoking an inflammatory reaction. [It should be noted that, although SDV1a required a 10-fold higher dose to achieve the same degree of chemotaxis in vitro—consistent with its 10-fold lower signaling based on  $\text{Ca}^{2+}$  efflux (Figs. 2 *B–D* and 3*C* and *SI Appendix, Fig. S5*)—the logistics of administering what is still a very small volume dose (1 to 2  $\mu$ L in an adult rodent), given the absence of adverse effects (see below), was deemed trivial and minimally invasive.] To make our observations unambiguous and minimize confounders, we first tested SDV1a under very stringent conditions, in the uninjured, nonpathologic adult mammalian brain, which normally does not

support extensive migration of NSCs (6, 8) (Fig. 2). We asked whether SDV1a injected into the adult murine cortex (we treated two separate cortical regions to avoid unwittingly choosing a favorable location) or hippocampus would attract hNSCs transplanted at a distance: For example, into the contralateral hippocampus, a site of adult rodent neurogenesis that might theoretically prompt hNSCs to resist the pull of the peptide. SDV1a did, indeed, attract the hNSCs to all regions where it was injected (Fig. 4, *Left*, regions *i–iii*), in contrast to injected PBS (a sham negative control for ruling out the effect of tissue damage from needle insertion alone), which drew no hNSCs (Fig. 4, *Right*, regions *i–iii*), and in contrast to recombinant CXCL12, which also, surprisingly, drew no hNSCs (for reasons explained below), yielding a picture identical to Fig. 4, *Right*, regions *i–iii*. Other comparisons with CXCL12 were also striking, as described below.

To provide more detail, 2 wk postengraftment transplanted hNSC-derived cells (as detected by human-specific mitochondrial [hMito] immunoreactivity) (1) were abundantly and widely distributed throughout the cortical parenchyma and hippocampus contralateral to their implantation site, congruent with SDV1a's distribution (detailed below) (Figs. 3*A* and 4, *Left*), and persisted throughout the lifetime of the mouse, indicating that the synthetic agonist SDV1a had successfully drawn the hNSCs to the targeted area where it had been administered, overcoming barriers to NSC migration. (The differentiation fate of engrafted hNSCs is more extensively explored below and in Fig. 8 and *SI Appendix, Fig. S9*). Nearly all implanted hNSCs migrated toward the SDV1a injection site in the contralateral hemisphere, with negligible (if any) remaining and integrating at the point of implantation on the side opposite to that of the SDV1a injection. With an engraftment efficiency of  $\sim 50\%$  for hNSCs in the telencephalon [as previously reported (4)], the expected  $\sim 1.0 \times 10^5$  donor-derived hMito<sup>+</sup> cells were appreciated throughout contralateral regions *i* to *iii* (Fig. 4, *Left*), the same regions *i* to *iii* demarcated in Fig. 5*A* as SDV1a's distribution (see below for greater detail).

If hNSCs were pretreated prior to transplantation with either a CXCR4 inhibitor (AMD3100) (31) or a CXCR7 inhibitor

**Fig. 5.** SDV1a's chemoattraction for hNSCs is CXCR4-specific, stable, persistent, widespread, and benign, provoking no inflammatory reactive microgliosis. (A) SDV1a persists in vivo in a widespread distribution for 3 wk postinjection. SDV1a was tagged with either FITC (green fluorescence) (Left) or biotin (revealed by reaction with Avidin-HRP to produce a brown precipitate) (Right), magnified in the respective Insets). SDV1a was injected into the regions shown in the schematics. Three weeks later, the brains were analyzed for persistence of the widely distributed SDV1a, as visualized by the tags. Representative photomicrographs are shown from the corresponding regions indicated in the schematic. SDV1a was detectable in all injected regions up to 3 wk postadministration as indicated by either green fluorescence (all cells in the field shown by a blue DAPI nuclear stain) (Left) or by a brown precipitate (all cells in the field seen as purple on this H&E stain) (Right). The distribution of the engrafted hNSCs in Fig. 4, Left, was congruent with the distribution of SDV1a as detected here. The hNSCs persisted for the lifetime of the animal although the peptide disappears after 3 wk. (Scale bars, 25  $\mu$ m.) (B) Blockade of CXCR4 (Left), but not of CXCR7 (Right), on transplanted hNSCs inhibits their migration toward SDV1a. Arrows in the schematic indicate sites of hNSC and SDV1a injections. Prior to transplantation, the hNSCs were preincubated *ex vivo* with either the CXCR4 inhibitor AMD3100 (Left) or the CXCR7 inhibitor CXCR7i (Right), exposure to which continued for 24 to 72 h postgrafting in vivo via an osmotic pump implanted at the site of transplantation. As early as 3 d posttransplant, hNSCs treated with the CXCR7 inhibitor had nevertheless migrated entirely to the contralateral side (hippocampus in this case), as indicated by the presence of hMito<sup>+</sup> cells (red) (Right) (similar to Fig. 4, Left); arrow indicates one such cell. In contrast, no hNSCs treated with the CXCR4 blocker were detectable there (Left), indicating that CXCR4 inhibition blocked the migration of engrafted hNSCs toward the SDV1a sites in mouse brain. As expected, no hNSCs were seen when PBS was injected instead of SDV1a as a sham control. All cells in the field are visualized by a DAPI (blue) nuclear stain. (Scale bars, 10  $\mu$ m.) These data suggested that SDV1a was acting highly specifically through CXCR4 directly on the hNSCs and not through other chemokine receptors or through intermediaries (e.g., receptors on macroglia, microglia, extracellular matrix, vascular endothelia, and so forth). (C) Brains treated with CXCL12/SDF1 $\alpha$  (Right) but not those treated with SDV1a (Left) engendered widespread abundant activated microgliosis. Activated M1 microglia are shown here as immunopositive for CD11b (red), but were similarly detected by antibodies to F4/80, CD68, and Iba1. Such microgliosis persisted as long as 2 wk postinjection. The Inset shows a high-power view from the field (white arrow) of a typical activated M1 microglial cell. The region shown (i in the schematics) in both conditions is representative of all areas exposed to SDV1a vs. CXCL12. An average of  $11.7 \pm 2.8$  per  $0.4 \text{ mm}^2$  CD11b<sup>+</sup> cells were present following an injection of native CXCL12 compared to only  $1.1 \pm 1.0$  CD11b<sup>+</sup> cells per  $0.4 \text{ mm}^2$  following an injection of SDV1a (a number comparable to the healthy adult murine brain). All cells in the field are visible by the DAPI (blue) nuclear stain. (Scale bars, 10  $\mu$ m; 5  $\mu$ m in the Inset). (*n* = 3 mice in each condition) (See also Fig. 7B for a similar demonstration of a lack of activated microgliosis in response to SDV1a.).



(CXCR7i) (the latter representing another chemokine receptor for CXCL12), hNSC migration to SDV1a was abrogated only with the former (Fig. 3B), suggesting that SDV1a was acting highly specifically through CXCR4 directly on the hNSCs and not through other cytokine receptors or through intermediaries (e.g., receptors on macroglia, microglia, extracellular matrix, vascular endothelia, and so forth).

Interestingly, as noted above, injection of exogenous recombinant human CXCL12 using the same procedure did not trigger comparable hNSC migration. An explanation for this difference may be found in the distribution and persistence of SDV1a compared to that of recombinant CXCL12. The cortical location of the engrafted hNSCs in response to SDV1a was, as noted above, congruent with SDV1a's distribution as detected by FITC-labeled SDV1a (Fig. 5A, Left) and biotinylated SDV1a (Fig. 5A, Right), which persisted for 3 wk postadministration. In contrast, recombinant CXCL12, similarly labeled, was undetectable by 2 d postadministration. This greater stability and persistence of SDV1a compared to recombinant CXCL12 might be attributable to its greater resistance to *in vivo* enzymatic degradation compared to CXCL12 (18) because of its unnatural amino acid composition; all amino acids in the DV1 binding motif are in a D-chirality. This short half-life for natural endogenous CXCL12 is transiently compensated for *in vivo* immediately following an injury by its being replenished recurrently by reactive astrocytes and vascular endothelium, as we previously reported (8); however, therapeutically, one could not—nor want to—rely on this mechanism for renewal.

The pharmacokinetics of SDV1a was consistent with rapid dissemination (by 30 min postinjection) throughout the regions illustrated in Fig. 4, *i-iii* and 5A with a  $C_{\max}$  of  $11.3 \pm 1.3 \mu\text{M/gm}$  of brain tissue.

SDV1a's persistence may also be ascribed to another striking difference between brains injected with SDV1a compared to those that received CXCL12 (and, indeed, one of our goals): The diminished degree of activated microgliosis engendered by the former compared to the latter. As suggested by SDV1a's induced gene-expression profile with a much reduced inflammatory signature (SI Appendix, Figs. S6 and S7), SDV1a evoked little, if any, microglial reactivity (Fig. 5C, Left), hence triggering fewer counteractive host responses to eliminate an "inciter." Microglia are early sensors of pathology and thus are the principal cellular mediators of inflammation in the brain. Activated resident microglial cells and recruited macrophages from the vascular compartment generate toxic products, such as oxygen-free radicals, nitric oxide, and neurotoxic cytokines (e.g., TNF- $\alpha$ , MIP1 $\alpha$ , and IL-1 $\beta$ ). Hence, monitoring the appearance of activated microglia is an excellent bellwether of an inflammatory milieu. The brains of mice receiving CXCL12 were characterized by a vast reactive M1 microgliosis [as determined not only by their immunostaining for CD11b, F4/80, CD68, and Iba1, but also by their activated and amoeboid morphology (42)] (Fig. 5C, Right). In stark contrast, there was virtually no microgliosis appreciated following injection of SDV1a despite its extensive contemporaneous chemoattractive pull on the hNSCs (Fig. 5C, Left). As in

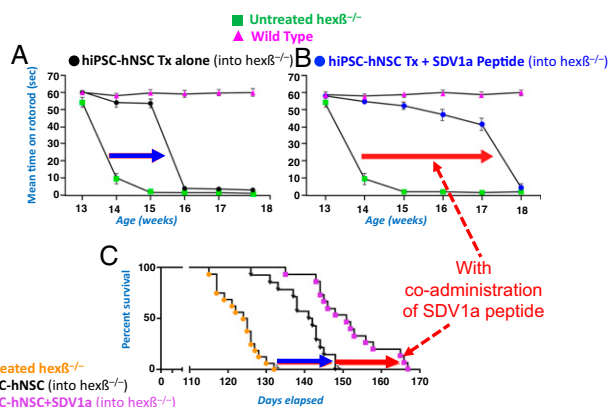


**Fig. 6.** Transplantation of hiPSC-derived hNSCs into the brains of Sandhoff ( $Hex\beta^{-/-}$ ) mice prolonged life, delayed onset of symptoms, and preserved motor function most significantly when grafting was accompanied by co-administration of SDV1a to insure distribution of Hex-producing cells throughout the mutant cortex. (A) Motor function deteriorated (as measured by rotarod) in 3-mo-old untreated Sandhoff disease mice (green squares,  $n = 14$ ). While the intraventricular transplantation (Tx) of hiPSC-hNSC forestalled symptomatic collapse by  $\sim 2$  wk (black circles,  $n = 22$ ;  $P < 0.001$  by  $t$  test compared to untreated Sandhoff disease mice), this period was significantly less than the 4-mo symptom-free period we previously reported using primary CNS- and hESC-derived hNSCs (1). (Data represent mean  $\pm$  SEM). hiPSC-derived hNSCs are known to have more limited migratory ability. However, coadministration of the hiPSC-hNSCs and the SDV1a peptide (B) forestalled loss of motor function until at least 4 mo with no significant decline until 18 wk in transplanted Sandhoff disease mice (blue circles,  $n = 14$ ) [ $P < 0.001$ ,  $t$  test compared to hiPSC-hNSC Tx  $Hex\beta^{-/-}$  mice without SDV1a (black circles) and compared to control untreated  $Hex\beta^{-/-}$  mice (green squares); mean  $\pm$  SEM]. Performance of WT mice is shown as pink triangles ( $n = 12$ ). (C) Survival (shown as Kaplan–Meier curves) of hiPSC-hNSC-transplanted Sandhoff disease mice without (black triangles,  $n = 22$ ) and with (purple squares,  $n = 14$ ) coadministration of SDV1a compared with untreated  $Hex\beta^{-/-}$  mice (orange circles,  $n = 14$ ). While hiPSC-hNSC transplanted Sandhoff disease mice without SDV1a did survive  $\sim 3$  wk longer (to 150 d) ( $P < 0.0001$ , log rank test), those coadministered with SDV1a at the time of the hiPSC-hNSC transplant had a much longer life span, by  $\sim 1.5$  mo to 5.5 mo ( $P < 0.0001$ , log rank test), a survival similar to that reported for CNS- and hESC-derived hNSCs (1). All hiPSC-hNSC transplanted Sandhoff disease mice were alive when all untreated Sandhoff disease mice had already died (131 d). Fibroblast transplantation yields survival and function curves indistinguishable from untreated Sandhoff disease mice, as we previously reported (1).

previous studies (1–5, 43), transplanted NSCs themselves do not provoke an inflammatory reaction, even without immunosuppression, likely because—at the differentiation state at which the cells are implanted—they do not express MHC class II (43). Mice were entirely normal histologically, physiologically, and behaviorally. (Note that, in these experiments in healthy adult mice, the blood–brain barrier was intact; the needle itself was so fine and applied so noninvasively that not even local trauma was induced by the injection. Therefore, infiltration of inflammatory cells from the peripheral circulation, such as lymphocytes and macrophages, would not be expected.)

Despite its wide distribution and long-term stability in recipient brains, SDV1a did not disrupt the blood–brain barrier; cause host cell death, abnormal host cell proliferation, distortion of host cytoarchitecture, or tumor formation; draw cells into the brain that do not belong there (including peripheral blood macrophages); or traffic to other organs, such as kidney, liver, lung, or spleen. Mice showed no evidence of systemic or CNS toxicity or altered behavior. As explored in greater detail below (and in Fig. 8 and *SI Appendix, Fig. S9*) the differentiation fate of hNSCs was unaltered, including, where appropriate, into electrophysiologically active neurons. Importantly, as noted above on

a cellular level for hNSCs (*SI Appendix, Figs. S6 and S7*), SDV1a did not induce a proinflammatory gene-expression profile within the adult mouse brain as a whole, in contrast to injected recombinant CXCL12, which did promote such a profile. In other words, injection of SDV1a, whether in conjunction with hNSC transplantation or alone, produced no inflammation. Interestingly, in the uninjured adult murine brain, SDV1a alone did not appear to draw endogenous host murine CXCR4-expressing cells to its location (the number of such cells in the SDV1a-injected cortex or hippocampus did not differ from that in the corresponding uninjected contralateral structure of the same mice or in homotopic regions of age-matched uninjected mice). The explanation for an absence of any redistribution of endogenous neural cells seemed simply to be that, in the intact adult mouse brain parenchyma, the cells expressing CXCR4 are not migratory NSCs, but rather well-integrated mature neural cells, largely neurons (*SI Appendix, Fig. S8*); in fact, the endogenous Nestin<sup>+</sup> NSCs in the adult brain parenchyma did not express CXCR4 (*SI Appendix, Fig. S8*). A rigorous study of this phenomenon of differential CXCR4 expression by cells of different phenotypes and different developmental ages in different brain regions under different conditions is beyond the scope of this paper; suffice it to say, this relatively selective effect of SDV1a in hNSC transplantation paradigms may further support its safety profile. In the disease model we describe below (Figs. 6–8 and *SI Appendix, Fig. S9*), SDV1a’s use (including any changes on endogenous cells below our level of detection) enhanced—and in no way hindered—the efficacy of a cell based-therapy.

Persistence of SDV1a in the CNS parenchyma, taken together with slow hNSC CXCR4 receptor turnover, strong affinity for the CXCR4 binding pocket, and a benign noninflammatory surrounding milieu, likely accounted for the stable presence of donor hNSCs in response to SDV1a, even in a typically non-neurogenic, nonmigration-supporting region. The instability of recombinant CXCL12 in a physiological environment (8, 41, 42), either because of its enzymatic degradation or the toxic inflammation it engenders, likely explains why it did not promote similar long-distance donor hNSC migration and integration within the host cortex.

#### Coadministration of SDV1a with hiPSC-Derived hNSCs Renders Them more Therapeutic.

We next determined whether such properties would enable SDV1a to circumvent a therapeutic obstacle. A long-standing challenge to regenerative medicine has been enhancing and directing the migration of therapeutic cells to regions in need (11, 12). (This obstacle has recently become particularly salient with the recognition that, for unknown reasons, hiPSC derivatives, although gaining in popularity for therapeutic transplants, migrate poorly compared to their primary or human embryonic stem cell [hESC] counterparts.) To assess whether a “chemo-mimetic” strategy could address this challenge, we elected to approach a disease model in which unambiguous measures of therapeutic success: 1) Pivot on adequate migration of hNSCs from their site of implantation to distant regions mediating key functions (e.g., the cortex); 2) demand wide-spread dissemination and integration of donor cells in those regions to affect improvement, and where the degree of benefit correlates with the extent of migration and integration of donor cells; 3) require that inflammation not be exacerbated, given that a prominent inflammatory signature already contributes to the pathophysiology; and 4) constitutive, spontaneous migration of grafted cells is limited. LSD mouse models nicely fit these criteria (1, 38). Indeed, lack of efficacy in some stem cell-based clinical trials for neuropathic LSDs have been attributed, in part, to inadequate coverage of diseased terrain by transplanted corrective cells (32). Furthermore, given the recently reported toxicity of viral vectors, such as AAV9, at



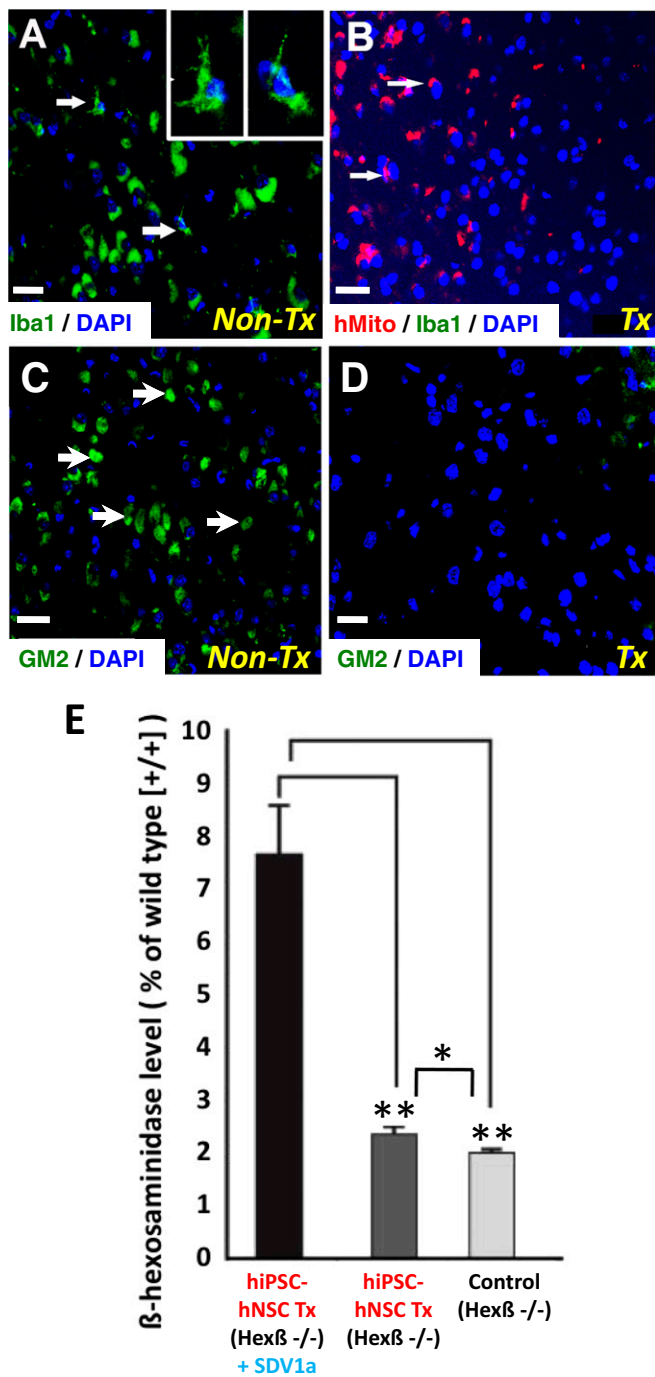


**Fig. 7.** hiPSC-hNSC-mediated mechanisms of improvement (enhanced by SDV1a) remain like those of other hNSCs (1): Enzyme replacement, GM2 ganglioside storage reduction, and suppression of inflammation. (A) Sandhoff disease is characterized by an intense activated microglia, as demonstrated by the density of cells expressing the M1 microglial marker *Iba1* (green, arrows) in the cortex of this representative untransplanted (non-Tx) 4-mo-old Sandhoff disease mouse. (*Iba1*<sup>+</sup> cells indicated by the arrows are magnified in the *Inset* to better visualize their microglial morphology). (B) In contrast, in age-matched Sandhoff disease mice that received hiPSC-hNSCs transplanted (Tx) into the cerebral ventricles and SDV1a coadministered into the cortex, wherever engrafted donor-derived cells were present (as confirmed here by their immunoreactivity to an antibody against hMito; red, white arrows), such microglia was scant. (The distribution of the donor hNSC-derived hMito<sup>+</sup> cells was like that shown in Fig. 4). (Scale bars in A and B, 20 μm; in *Inset*, 5 μm.) (C) Representative confocal photomicrograph showing significant amounts of immunoreactive GM2 ganglioside storage (green, arrows) in the same cortical region shown

the high doses required for widespread CNS gene replacement (33), cell-based gene therapy will likely play an even more prominent role in these conditions.

Of the neuropathic LSDs, we elected to approach Sandhoff disease (1) not only because this lethal neurodegenerative disorder provides a stringent, rapid, and unambiguous test for a tool to enhance stem cell migration and chimerism, but also because we have a rich database on this model, having studied it extensively (1). In addition, the largely invariant natural history of patients with this condition (for which the mouse model is excellently representative) is well-established. Sandhoff disease is a rapidly progressive lethal neurodegenerative condition characterized by a deletion mutation of the gene encoding the β-chain of the secreted diffusible lysosomal enzyme β-hexosaminidase (Hex), leading to absence of both its dimeric isoforms, Hex A and Hex B. This complete absence of Hex results in intra-neuronal ganglioside storage and inflammation, leading to inexorable neuronal death and neurological demise.

We previously reported (1) that exogenous normal hNSCs—whether derived from hESCs or isolated directly from the CNS—when transplanted into the cerebral ventricles of newborn Sandhoff disease (*Hexβ*<sup>-/-</sup>) mice, integrated into the sub-ventricular zone and, from there, migrated extensively throughout the brain, forestalling disease onset, preserving function, and substantially extending life. We profiled the multiple mechanisms by which hNSCs imparted this benefit (4): 1) They constitutively produced Hex A and B, which was endocytosed by mutant cells via their mannose-6-phosphate (M6P) receptor, restoring normal metabolism; 2) they reduced ganglioside storage within host neurons by virtue of this cross-correction; 3) they replaced a small number of degenerating neurons as well as glia; and 4) they diminished inflammation. The success of these actions was dependent on widespread dissemination and integration of the exogenous NSCs, particularly in the cortex where a threshold density of donor-to-host cells was required: A 1:10 ratio conferred whole-brain Hex activity that was >3 to 5% of WT, a threshold level sufficient to restore normal metabolism (1), even achieving levels as high as 28% of WT Hex activity in areas of densest hNSC chimerism (4). hNSCs derived from hiPSCs (44) have not yet been tested in this model, although our expectations were modest given the growing concern regarding hiPSC migration. Normally, for a monogenic disease, one would not want to use autologous cells for a cell-based treatment given that those cells also bear the enzyme deficiency. However, the potential appeal of patient-specific hiPSCs in this situation, particularly in view of the latter-day ease of correcting monogenic defects by either genome editing or virus-mediated transgene transfer, was that immunocompatible hiPSCs could be re-injected periodically throughout a patient's life as the brain grows or donor-derived cells die without the risk of immunorejection. A first

in A from the same representative 4-mo-old untransplanted Sandhoff disease mouse. (D) In contrast, little GM2 accumulation occurred in the same region of an age-matched Sandhoff disease mouse transplanted (Tx) with hiPSC-hNSCs coadministered with SDV1a (same mouse and region as in B). DAPI nuclear stain (blue) marked all cells shown. (Scale bar, 20 μm.) The images in A–D are orthogonal projections composed of 9 to 16 optical z-planes of thickness 0.5 to 1 μm. *n* = 6 animals per experiment group. (E) To provide a mechanistic basis for the observations in A–D, we demonstrated that Hex enzyme levels in the CNS parenchyma of Sandhoff disease mice were raised beyond the critical 3 to 5% therapeutic threshold in regions where donor cells were attracted by SDV1a to integrate as opposed to regions where they were not (i.e., transplanted but without SDV1a coadministration). The Hex levels in the hiPSC-hNSC+SDV1a Sandhoff disease mice were significantly higher than those in SD mice transplanted but without SDV1a or in untransplanted Sandhoff disease mice (\**P* < 0.05, \*\**P* < 0.01 by two-tailed *t* test). The donor-to-host cell ratio in engrafted regions was 1:10, as previously reported (1).

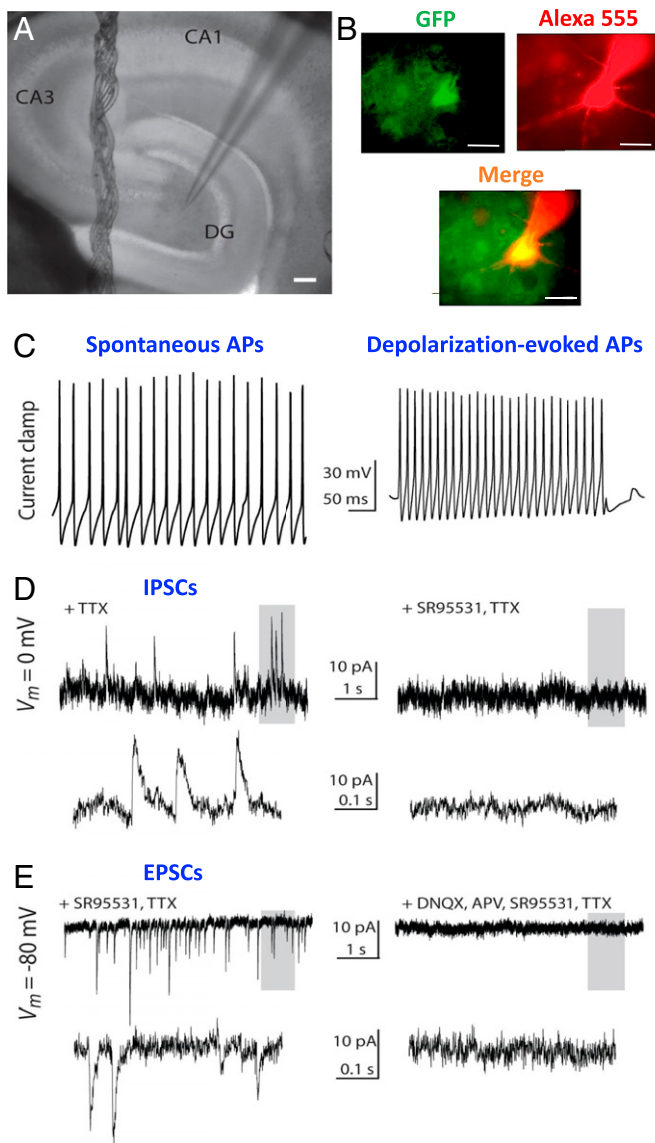


**Fig. 8.** Fate of the donor-derived hiPSC-hNSCs in vivo not compromised when coadministered with SDV1a. Although the most dominant mechanisms for improving survival and function (as in Fig. 6) are cell-mediated provision of Hex (Fig. 7E), reduction in host intracellular GM2 accumulation (Fig. 7C and D), and blunting microgliosis (Fig. 7A and B), we also confirmed the integration of hiPSC-hNSC derivatives into the host cytoarchitecture in a functionally and cell-type appropriate manner in conjunction with the administration of SDV1a. A more complete survey is provided in *SI Appendix, Fig. S9*. Shown here is the demonstration that neurons derived from hiPSC-hNSCs are electrophysiologically active and receive both excitatory and inhibitory synaptic inputs. (A) Low-power image of hippocampus showing the location of a representative recorded cell. Hippocampal subfields are labeled: dentate gyrus (DG), CA3, and CA1. (B) Fluorescence images of a recorded eGFP<sup>+</sup> donor-derived cell (green) in a cortical slice from a representative 2-mo-old *Hexβ*<sup>-/-</sup> mouse engrafted with eGFP-expressing hiPSC-hNSCs at birth with coadministered SDV1a. The cell has been filled by Alexa 555 (red) in the recording pipette. Note the filled neurites extending from the cell body. Recordings from this cell are shown in C–E. (Scale bars, 100 μm for A, 40 μm B.) (C, Left) Current-clamp recording of an eGFP<sup>+</sup> cell showing spontaneous action potentials (APs). (C, Right) Recording from the same cell with APs produced by injecting depolarizing current. (D, Left) Voltage clamp recording in tetrodotoxin (TTX), a Na<sup>+</sup> channel blocker, to suppress APs and hold the cell at 0 mV to eliminate excitatory synaptic currents and allow visualization of spontaneous inhibitory postsynaptic currents (IPSCs). Upper traces are shown at a compressed timescale. The trace framed by the gray boxes are expanded in the Lower trace. (Right) A demonstration that IPSCs can be eliminated by washing in SR95531, a

transplant, even with allogeneic NSCs (as we reported in newborns and adults) does not require immunosuppression (1, 3, 43); however, subsequent reimplantation of the same NSCs does run the risk of rejection based on prior sensitization. Hence determining the efficacy and safety of hiPSCs for this condition seemed justified.

The consensus view is that, when using NSCs to address a global encephalopathy requiring extensive chimerism, instillation into the cerebral ventricles (particularly of newborn or juvenile brains), is superior to multiple intraparenchymal injections for minimizing invasiveness while maximizing efficacy (1, 38). (Intravascular routes have not been successful for enzyme or cell replacement in this neuropathic LSD.) It initially seemed trivial to replicate our previously reported intraventricular approach (1, 38), now simply using hNSCs derived from normal hiPSCs, neuralized according to well-accepted published protocols (34, 45). However, such hiPSC-derived hNSCs (hiPSC-hNSCs), as feared, were more limited in their migratory capacity compared to primary CNS- and hESC-derived hNSCs (1), an observation suggested by others (46, 47). In our case, the hiPSC-derived hNSCs did not migrate to the cortex from their implantation site in the ventricles, severely limiting their efficacy for Sandhoff disease. In other words, although engrafted Hex-expressing hiPSC-derived hNSCs did increase life span and improve motor function of the Sandhoff disease mice somewhat (Fig. 6), their impact was inferior to that from primary CNS- and hESC-derived hNSCs (4) due to their limited migration from periventricular regions to the cortex. This limitation was replicated using different hiPSC lines from different suppliers neuralized using different accepted protocols (*SI Appendix, Detailed Experimental Procedures*). We viewed it as beyond the scope of this work to determine the reason for this more limited migration. It may represent a component of residual epigenetic memory or the consequences of the genetic manipulation inherent in reprogramming; suffice it to say that, in using accepted and oft-used published generation and differentiation protocols, we eliminated “technique” as a confounder. Rather, we accepted this consistent observation by us and others (46, 47) of restricted migration as a potential limitation to hiPSC-based therapies for these types of neural transplantation challenges, and rather viewed this obstacle as an opportunity to demonstrate that a synthetic chemokine agonist could effectively optimize the impact of cell-based therapies by enhancing migration (a demanding proof-of-concept).

Indeed, when hiPSC-derived hNSCs were implanted into the cerebral ventricles of neonatal *Hexβ*<sup>-/-</sup> mouse brains contemporaneously with the minimally invasive administration of 1 μL of 3.2 μM SDV1a into each hemisphere’s superficial dorsal cortex via a finely drawn glass micropipette (by barely puncturing the meninges, as we had done with normal adult mice in Fig. 4), we now observed wide dissemination of corrective donor-derived neural cells (which constitutively expressed fully assembled and active Hex A and B) throughout the diseased brain (1) (Fig. 7; and as per Fig. 4) with a significant therapeutic impact, now comparable to what we previously reported for other sources of hNSCs (1). This impact included delayed disease onset, preserved motor-function [as assessed by rotarod (1, 2)], prolonged symptom-free survival, and extended lifespan (Fig. 6). Hex activity was now measurable throughout the cortex (Fig. 7, histograms) with the donor-to-host cell ratio cited above, as we previously reported (4); host intraneuronal glycosphingolipid (GSL) monosialoganglioside (GM2) storage was reduced at 2-mo of age (as measured using the standard biochemical reaction, immunohistochemistry,

GABA<sub>A</sub> receptor antagonist. (E, Left) Same cell as in D, held at –80 mV to reveal excitatory postsynaptic currents (EPSCs). (Right) A demonstration that EPSCs can be eliminated by DNQX and APV, AMPA and NMDA receptor blockers, respectively.

and HP-TLC) compared to untransplanted age-matched *Hexβ*<sup>-/-</sup> littermates, as well as *Hexβ*<sup>-/-</sup> littermates transplanted without coadministration of SDV1a (Fig. 7). No GM2 was detected in normal mouse brains (Fig. 7 C and D). In addition, inflammation within the *Hexβ*<sup>-/-</sup> cortex was actually diminished [attributable to the previously documented (1, 2, 38) and now well-accepted immunomodulatory actions of hNSCs (5)] with no additional inflammation or microgliosis having been induced by the SDV1a (Fig. 7 A and B). Furthermore, SDV1a did not antagonize the antiinflammatory actions of the hNSCs.

Five percent ( $\pm 1\%$ ) of donor-derived hNSCs differentiated into neurons in the cortex with appropriate electrophysiological properties (Fig. 8), a proportion we had similarly observed for primary CNS-derived and hESC-derived hNSCs (1). Although such neurons were not central to the therapeutic impact of the hiPSC-hNSCs in this disease model, their presence reaffirmed that SDV1a did not alter the differentiation profile of hNSCs, or the ability of their derivatives to integrate into host cytoarchitecture in a functionally and cell type-appropriate manner, or their mechanisms-of-therapeutic-action in the Sandhoff disease mouse model. All SDV1a appeared to change was the distribution of the implanted hiPSC-derived hNSCs, allowing them to cover, and hence rescue, a broader critical terrain of mutant brain, thus enhancing the hiPSC-derived hNSC's therapeutic impact on this disease.

For completeness, we found that the remainder of the hiPSC-hNSC differentiation pattern in the engrafted SDV1a exposed brains ( $n = 35$ ) was also similar to what we previously reported for primary CNS- and hESC-derived hNSCs (4) (39% expressing astroglial markers, 2% oligodendroglial markers, 54% markers of undifferentiated neural progenitors) (SI Appendix, Fig. S9). No other cell types (including nonneural lineages) were represented. All cells expressed Hex. No tumors, cell overgrowth, distortion of host cytoarchitecture, or hemorrhages were observed. (Although beyond the scope of this study, an effective long-term cell-based treatment of this condition may entail periodic readministration of hiPSC-derived neural cells at cardinal time points throughout a patient's life when Hex levels dip below a certain threshold or symptoms recur as the brain grows and WT cells senesce and die.)

## Discussion

In summary, we have explored a strategy for directing the migration of transplanted stem cells, particularly hiPSC-derived hNSCs, by harnessing one of stem cell biology's fundamental actions, pathotropism, as mediated by inflammatory chemokine-receptor interaction. As proof-of-concept that one can develop a bifunctional ligand that divorces inflammatory signaling from migratory signaling as well as from binding, we developed, through chemical mutagenesis of the prototypical cytokine CXCL12, a "dual-moiety" prototypic synthetic CXCR4 agonist peptide that contains a maximal selective receptor binding motif linked to a modified and shortened CXCR4-activating motif of higher signaling specificity. We documented significant advantages of the synthetic agonist over recombinant versions of the natural CXCR4 agonist CXCL12 in the mouse brain in terms of distribution, stability, inflammogenesis, duration of chemoattraction and, most importantly, extent and success of migratory guidance of engrafted CXCR4-expressing stem cells, such as hNSCs. As evidence of its translational value, we used the peptide to guide engrafted hiPSC-derived hNSCs, whose own migratory repertoire appears limited, toward sites of CNS pathology, alleviating symptoms, preserving function, and prolonging life in a mouse model of a prototypical neurodegenerative disorder. Importantly, microgliosis and inflammation were actually suppressed, not provoked; that is, the antiinflammatory action of the hNSCs was not contravened by the CXCL12-mimetic as might have been feared. (In many neurodegenerative diseases there is strong evidence for an inflammatory response initiated

by microglial activation leading to neuronal apoptosis.) To our knowledge, this synthetic chemokine agonist designed, characterized, and validated in a translationally relevant system is unique. [Of note, one would actually not want to test this phenomenon in an acute focal traumatic injury model because, as we've previously shown (2–5, 48), migratory signals from a reservoir of concentrated inflammatory cues, as in the epicenter of a circumscribed lesion, already abets likely adequate migration, although one could certainly optimize it with this peptide. One wants to test proof-of-concept in a dramatically deficient model, as we've done here.]

Since CXCR4 is present on most stem cells in most organs, SDV1a could be useful outside the nervous system as well for directing stem cells from a range of derivations for many pathological conditions (5–12, 49–54). Furthermore, because signaling between CXCL12 and CXCR4 is an oft-explored axis, having been implicated in a number of degenerative CNS diseases and other disorders (5–12, 49–54), the agonist may be useful as a molecular probe for further understanding ligand-GPCR signaling in studying pathogenic mechanisms (21). Additionally, this approach of subjecting inflammatory chemokines to chemical mutagenesis to maximize desirable properties (e.g., homing) and minimize undesirable characteristics (e.g., inimical inflammatory reactions) could be applicable to other chemokines. Other chemokine receptors are thought to have a two-site interaction with their ligand similar to that we exploited for CXCR4 (18–20). Moreover, many of these sites are druggable.

In short, off-the-shelf, reasonably priced, broadly applicable chemokine analogs and chemokine-receptor agonists with in vivo stability, potent chemoattraction without inflammogenesis or adverse off-target actions, and with established efficacy, efficiency, tolerability, and safety in pathologic conditions requiring a specific distribution and location of therapeutic cells should provide regenerative medicine with another tool. In the CNS, one might envision using such a novel GPCR-targeted medication when reparative stem cells (producing therapeutic molecules, scavenging or neutralizing toxins, enhancing remodeling, providing therapeutic structures like myelin, or replacing cells) must: 1) Be directed to needed regions (e.g., the cortex in dementing disorder); 2) be more widely distributed to broaden their chimerism (e.g., throughout the spinal cord in neuromuscular diseases, such as amyotrophic lateral sclerosis); 3) be more homogeneously distributed within a given organ to avoid overly concentrated niduses of cells (e.g., dopamine-expressing cells in the striatum of Parkinsonian patients); 4) have a permissive milieu recreated for them within chronically injured microenvironments where proreparative cues have abated. In addition, blunting undesirable signaling as we did here may be useful in other systems: For example, chimeric antigen receptor T-cell antineoplastic immunotherapy in order to minimize the adverse effects of cytokine ("storm") release syndrome (55, 56).

## Methods

To synthesize SDV1a, the first 21 amino acids (all in a D-chirality) from the N-terminal of the CXCR4 antagonist vMIP-II were inserted in place of CXCL12's proximal N terminus to provide a ligand with the highest affinity for the binding pocket. The distal N-terminal signaling motif of CXCL12, which engages the signaling pocket, was truncated to the first 8 amino acids, narrowing the spectrum of G protein-mediated pathways activated. After affirming SDV1a's specificity and efficacy in CXCR4 competition assays, it was injected into regions of normal adult mouse brain and of the brains of Sandhoff disease mice into which we cotransplanted hNSCs to home and engraft.

**Data Availability.** All study data are included in the article and supporting information. All materials and protocols are available from E.Y.S., Z.H., or J.-P.L.

**ACKNOWLEDGMENTS.** This work was supported by grants from the National Institutes of Health (R01-GM057761), the California Institute for Regenerative Medicine (RS1-00225-1), the Department of Defense (W81XWH-16-1-0087-02), the National Tay-Sachs & Allied Disease Foundation, the Children's Neurobiological Solutions Foundation.

1. J.-P. Lee *et al.*, Stem cells act through multiple mechanisms to benefit mice with neurodegenerative metabolic disease. *Nat. Med.* **13**, 439–447 (2007).
2. Y. D. Teng *et al.*, Multimodal actions of neural stem cells in a mouse model of ALS: A meta-analysis. *Sci. Transl. Med.* **4**, 165ra164 (2012).
3. K. S. Aboody *et al.*, Neural stem cells display extensive tropism for pathology in adult brain: Evidence from intracranial gliomas. *Proc. Natl. Acad. Sci. U.S.A.* **97**, 12846–12851 (2000).
4. K. I. Park *et al.*, Acute injury directs the migration, proliferation, and differentiation of solid organ stem cells: Evidence from the effect of hypoxia-ischemia in the CNS on clonal "reporter" neural stem cells. *Exp. Neurol.* **199**, 156–178 (2006).
5. J. Imitola *et al.*, Directed migration of neural stem cells to sites of CNS injury by the stromal cell-derived factor 1alpha/CXC chemokine receptor 4 pathway. *Proc. Natl. Acad. Sci. U.S.A.* **101**, 18117–18122 (2004).
6. A. Belmadani, P. B. Tran, D. Ren, R. J. Miller, Chemokines regulate the migration of neural progenitors to sites of neuroinflammation. *J. Neurosci.* **26**, 3182–3191 (2006).
7. M. Li, J. S. Hale, J. N. Rich, R. M. Ransohoff, J. D. Lathia, Chemokine CXCL12 in neurodegenerative diseases: An SOS signal for stem cell-based repair. *Trends Neurosci.* **35**, 619–628 (2012).
8. K. S. Carbajal, C. Schaumburg, R. Strieter, J. Kane, T. E. Lane, Migration of engrafted neural stem cells is mediated by CXCL12 signaling through CXCR4 in a viral model of multiple sclerosis. *Proc. Natl. Acad. Sci. U.S.A.* **107**, 11068–11073 (2010).
9. P. B. Tran, D. Ren, T. J. Veldhouse, R. J. Miller, Chemokine receptors are expressed widely by embryonic and adult neural progenitor cells. *J. Neurosci. Res.* **76**, 20–34 (2004).
10. Q. Ma *et al.*, Impaired B-lymphopoiesis, myelopoiesis, and derailed cerebellar neuron migration in CXCR4- and SDF-1-deficient mice. *Proc. Natl. Acad. Sci. U.S.A.* **95**, 9448–9453 (1998).
11. J. M. Karp, G. S. Leng Teo, Mesenchymal stem cell homing: The devil is in the details. *Cell Stem Cell* **4**, 206–216 (2009).
12. S. Khaldoyanidi, Directing stem cell homing. *Cell Stem Cell* **2**, 198–200 (2008).
13. M. P. Crump *et al.*, Solution structure and basis for functional activity of stromal cell-derived factor-1; dissociation of CXCR4 activation from binding and inhibition of HIV-1. *EMBO J.* **16**, 6996–7007 (1997).
14. N. Heveker *et al.*, Dissociation of the signalling and antiviral properties of SDF-1-derived small peptides. *Curr. Biol.* **8**, 369–376 (1998).
15. C. Z. Dong *et al.*, Different stereochemical requirements for CXCR4 binding and signaling functions as revealed by an anti-HIV, D-amino acid-containing SMM-chemokine ligand. *J. Med. Chem.* **48**, 7923–7924 (2005).
16. P. Palladino *et al.*, Structural determinants of unexpected agonist activity in a retropeptide analogue of the SDF-1alpha N-terminus. *FEBS Lett.* **579**, 5293–5298 (2005).
17. W. T. Choi *et al.*, Unique ligand binding sites on CXCR4 probed by a chemical biology approach: Implications for the design of selective human immunodeficiency virus type 1 inhibitors. *J. Virol.* **79**, 15398–15404 (2005).
18. S. Tian *et al.*, Distinct functional sites for human immunodeficiency virus type 1 and stromal cell-derived factor 1alpha on CXCR4 transmembrane helical domains. *J. Virol.* **79**, 12667–12673 (2005).
19. B. Wu *et al.*, Structures of the CXCR4 chemokine GPCR with small-molecule and cyclic peptide antagonists. *Science* **330**, 1066–1071 (2010).
20. N. Zhou, Z. Luo, J. Luo, J. W. Hall, Z. Huang, A novel peptide antagonist of CXCR4 derived from the N-terminus of viral chemokine vMIP-II. *Biochemistry* **39**, 3782–3787 (2000).
21. D. Wacker, R. C. Stevens, B. L. Roth, How ligands illuminate GPCR molecular pharmacology. *Cell* **170**, 414–427 (2017).
22. E. Lindahl, B. Hess, D. van der Spoel, GROMACS 3.0: A package for molecular simulation and trajectory analysis. *J. Mol. Model.* **7**, 306–317 (2001).
23. B. Hess, C. Kutzner, D. van der Spoel, E. Lindahl, GROMACS 4: Algorithms for highly efficient, load-balanced, and scalable molecular simulation. *J. Chem. Theory Comput.* **4**, 435–447 (2008).
24. A. D. Luster, Chemokines—Chemotactic cytokines that mediate inflammation. *N. Engl. J. Med.* **338**, 436–445 (1998).
25. W. T. Choi, S. Duggineni, Y. Xu, Z. Huang, J. An, Drug discovery research targeting the CXC chemokine receptor 4 (CXCR4). *J. Med. Chem.* **55**, 977–994 (2012).
26. N. Zhou *et al.*, Exploring the stereochemistry of CXCR4-peptide recognition and inhibiting HIV-1 entry with D-peptides derived from chemokines. *J. Biol. Chem.* **277**, 17476–17485 (2002).
27. D. Liu *et al.*, Crystal structure and structural mechanism of a novel anti-human immunodeficiency virus and D-amino acid-containing chemokine. *J. Virol.* **81**, 11489–11498 (2007).
28. T. N. Kledal *et al.*, A broad-spectrum chemokine antagonist encoded by Kaposi's sarcoma-associated herpesvirus. *Science* **277**, 1656–1659 (1997).
29. E. De Clercq, Inhibition of HIV infection by bicyclams, highly potent and specific CXCR4 antagonists. *Mol. Pharmacol.* **57**, 833–839 (2000).
30. N. Fujii, H. Tamamura, Peptide-lead CXCR4 antagonists with high anti-HIV activity. *Curr. Opin. Investig. Drugs* **2**, 1198–1202 (2001).
31. H. E. Broxmeyer *et al.*, Rapid mobilization of murine and human hematopoietic stem and progenitor cells with AMD3100, a CXCR4 antagonist. *J. Exp. Med.* **201**, 1307–1318 (2005).
32. StemCells Inc., StemCells Inc. announces termination of Phase II pathway study following review of data, <https://globenewswire.com/news-release/2016/05/31/844686/0/en/StemCells-Inc-Announces-Termination-of-Phase-II-Pathway-Study-Following-Review-of-Data.html> (2016). Accessed 2 November 2020.
33. C. Hinderer *et al.*, Severe toxicity in non-human primates and piglets following high dose intravenous administration of an AAV vector expressing human SMN. *Hum. Gene Ther.* **29**, 285–298 (2018).
34. S. M. Chambers *et al.*, Highly efficient neural conversion of human ES and iPS cells by dual inhibition of SMAD signaling. *Nat. Biotechnol.* **27**, 275–280 (2009).
35. W. Humphrey, A. Dalke, K. Schulten, VMD: Visual molecular dynamics. *J. Mol. Graph.* **14**, 33–38, 27–28 (1996).
36. R. L. Klemke *et al.*, Regulation of cell motility by mitogen-activated protein kinase. *J. Cell Biol.* **137**, 481–492 (1997).
37. D. C. Cara, J. Kaur, M. Forster, D. M. McCafferty, P. Kubas, Role of p38 mitogen-activated protein kinase in chemokine-induced emigration and chemotaxis in vivo. *J. Immunol.* **167**, 6552–6558 (2001).
38. J. D. Flax *et al.*, Engraftable human neural stem cells respond to developmental cues, replace neurons, and express foreign genes. *Nat. Biotechnol.* **16**, 1033–1039 (1998).
39. D. R. Wakeman *et al.*, Long-term multilayer adherent network (MAN) expansion, maintenance, and characterization, chemical and genetic manipulation, and transplantation of human fetal forebrain neural stem cells. *Curr. Protoc. Stem Cell Biol.* **Chap 2**, Unit2D 3, (2009).
40. G. D. Sharma, J. He, H. E. Bazan, p38 and ERK1/2 coordinate cellular migration and proliferation in epithelial wound healing: evidence of cross-talk activation between MAP kinase cascades. *J. Biol. Chem.* **278**, 21989–21997 (2003).
41. A. Mortier, J. Van Damme, P. Proost, Overview of the mechanisms regulating chemokine activity and availability. *Immunol. Lett.* **145**, 2–9 (2012).
42. S. Tanabe *et al.*, Functional expression of the CXC-chemokine receptor-4/fusin on mouse microglial cells and astrocytes. *J. Immunol.* **159**, 905–911 (1997).
43. J. Imitola *et al.*, Neural stem/progenitor cells express costimulatory molecules that are differentially regulated by inflammatory and apoptotic stimuli. *Am. J. Pathol.* **164**, 1615–1625 (2004).
44. B. T. D. Tobe *et al.*, Probing the lithium-response pathway in hiPSCs implicates the phosphoregulatory set-point for a cytoskeletal modulator in bipolar pathogenesis. *Proc. Natl. Acad. Sci. U.S.A.* **114**, E4462–E4471 (2017).
45. I. Singec *et al.*, Quantitative analysis of human pluripotency and neural specification by in-depth (phospho)proteomic profiling. *Stem Cell Reports* **7**, 527–542 (2016).
46. J. Ladewig, P. Koch, O. Brüstle, Auto-attraction of neural precursors and their neuronal progeny impairs neuronal migration. *Nat. Neurosci.* **17**, 24–26 (2014).
47. M. Czepiel, L. Leicher, K. Becker, E. Boddeke, S. Copray, Overexpression of polysialylated neural cell adhesion molecule improves the migration capacity of induced pluripotent stem cell-derived oligodendrocyte precursors. *Stem Cells Transl. Med.* **3**, 1100–1109 (2014).
48. A. Obenaus *et al.*, Long-term magnetic resonance imaging of stem cells in neonatal ischemic injury. *Ann. Neurol.* **2**, 282–291 (2011).
49. T. Pozzobon, G. Goldoni, A. Viola, B. Molon, CXCR4 signaling in health and disease. *Immunol. Lett.* **177**, 6–15 (2016).
50. J. X. Yang *et al.*, CXCR4 receptor overexpression in mesenchymal stem cells facilitates treatment of acute lung injury in rats. *J. Biol. Chem.* **290**, 1994–2006 (2015).
51. T. C. Tu *et al.*, A chemokine receptor, CXCR4, which is regulated by hypoxia-inducible factor 2a, is crucial for functional endothelial progenitor cell migration to ischemic tissue and wound repair. *Stem Cell Develop.* **25**, 366–376 (2016).
52. K. Tachibana *et al.*, The chemokine receptor CXCR4 is essential for vascularization of the gastrointestinal tract. *Nature* **393**, 591–594 (1998).
53. M. E. Mayorga *et al.*, Role of SDF-1: CXCR4 in Impaired post-myocardial infarction cardiac repair in diabetes. *Cell Translational Med.* **7**, 115–124 (2018).
54. R. M. Ransohoff, D. Schafer, A. Vincent, N. E. Blachère, A. Bar-Or, Neuroinflammation: ways in which the immune system affects the brain. *Neurotherapeutics* **12**, 896–909 (2015).
55. S. S. Neelapu *et al.*, Chimeric antigen receptor T-cell therapy — assessment and management of toxicities. *Nat. Rev. Clin. Oncol.* **15**, 47–62 (2018).
56. R. Channappanavar, S. Perlman, Pathogenic human coronavirus infections: causes and consequences of cytokine storm and immunopathology. *Semin Immunopathol.* **39**, 529–539 (2017).